Far-infrared, microwave, and inelastic neutron scattering experiments of the superionic conductor α-AgI

P. Brüesch
Brown Boveri Research Center, CH-5405 Baden-Dättwil, Switzerland

W. Bührer
Institut für Reaktortechnik ETHZ, c/o E.I.R., CH-5303 Würenlingen, Switzerland

H. J. M. Smeets
University of Nijmegen, Research Institute for Materials, Toernooiveld, Nijmegen, The Netherlands
(Received 5 September 1979)

New far-infrared, microwave, and inelastic neutron scattering experiments of the superionic conductor α-AgI are presented. As to the optical studies, far-infrared reflection and transmission spectra between 3 and 400 cm^{-1} in the temperature range between 20 and 440 °C have been measured. The far-infrared transmission data have been checked independently by microwave techniques in the frequency range between 2.5 and 8 cm^{-1}. The drastic increase in the absorption at the transition temperature and its relatively weak temperature dependence in the α phase is due to the almost complete disordering of the silver ions at the phase transition. Based on these experimental data the frequency-dependent conductivity of α-AgI has been evaluated. Besides the residual ray absorption near 110 cm^{-1} the conductivity is high down to 3 cm^{-1} with a second very broad resonance near 18 cm^{-1}. For the first time, inelastic neutron scattering experiments on a large single crystal of α-AgI have been performed. These measurements proved the lattice-dynamical origin of the absorption between 5 and 30 cm^{-1}. An extremely large linewidth for the transverse-acoustic phonon modes is observed. It is concluded that it is mainly the disorder of the silver ions which is responsible for this broadening.

I. INTRODUCTION

The superionic conductor α-AgI is one of the simplest and most famous solid electrolytes known. Many experimental and theoretical studies have been devoted to this outstanding silver ion conductor with the aim to get more insight into the lattice dynamics and conductivity mechanism.[1-5] In this paper, we present new experimental results, namely, optical experiments in the far-infrared and microwave region as well as inelastic neutron scattering experiments of single cyrstals of α-AgI. The results are discussed on the basis of recently developed models. As to the optical measurements, we present for the first time temperature-dependent reflectivity and transmission data between 400 and 3 cm^{-1} from which we deduce the frequency-dependent conductivity. From the observed temperature dependence important conclusions can be made as to the nature of the different absorption processes in the highly conducting phase. Much effort has been devoted to the technically difficult frequency regime between 2.5 and 10 cm^{-1}. Until now no reliable optical data have been available in this part of the spectrum. Physically, this frequency range is of great importance because it is the range in which the transition from the oscillatory motion ot the diffusive motion of the silver ions takes place. On the other hand, the frequency dependence of the conductivity is intimately linked to the lattice vibrations. By inelestic coherent neutron measurements the dispersion relation of acoustic-phonon modes has been determined. From the theoretical viewpoint, the lattice dynamics of α-AgI is complicated by both the disorder of the silver ions and the anharmonicity. By comparing the data of the high-temperature α phase with those of the low-temperature, ordered β phase, we obtain detailed information about the ionic motions in the disordered structure of α-AgI which elucidates the conductivity measurements.

II. FAR-INFRARED AND MICROWAVE EXPERIMENTS OF α- AND β-AgI

A. Far-infrared experiments

All far-infrared measurements have been performed with a Beckman FS 720 interferometer. For measurements above 150 cm^{-1} the instrument was used in the Michelson mode and below 150 cm^{-1} in the polarizing mode.[6] The polarizing interferometer which is working with corner reflectors and wire grid polarizer as beam divider efficiently suppresses the mean level of the interferogram. Since the mean level is a carrier of noise due to source fluctuations, vibrations of optical components, etc., this leads to a greatly improved signal-to-noise ratio. All mea-

surements have been performed with a dc mercury source. Both a Golay cell and a germanium bolometer operated at 1.5 K have been used as a detector. The low-frequency limit of the Golay cell is about 7–10 cm^{-1}, depending on the sample. It is well known that due to the extremely small output power of the source, measurements below 10 cm^{-1} are not an easy task. For studies at low frequencies a fluorogold filter with a cutoff frequency at 30 cm^{-1} was mounted in front of the germanium crystal of the bolometer. In addition, a standard far-infrared mesh interference filter from Cambridge Physical Sciences with a cutoff frequency at 10 cm^{-1} was used at very low frequencies. With these filters, together with the advantage of the polarizing mode, it was possible to measure down to 3 cm^{-1}. Most spectra have been obtained with a resolution of 0.6–1.2 cm^{-1}. The stability of the source and the bolometer have been checked by measuring the reference interferograms before and after the sample measurements which usually took about eight hours; no significant change in the intensity has been observed.

A specially constructed reflection and transmission cell has been used for this work, the details of which are described elsewhere.[7] The samples were heated by a central stream of hot nitrogen while the windows (sealed with normal *O* rings) were kept near room temperature by a peripheral cold stream of nitrogen. This guarantees a uniform temperature over the whole sample which is a great advantage as compared to the usual method where the sample is placed on a "hot finger." In fact, the latter method leads to temperature differences between the hot finger and the reflecting surface of as high as 100 °C in the case of thick AgI pellets. In order to avoid the disturbing reflectivity from the windows, oblique windows have been used for all reflectivity measurements. The sample holder carrying the sample and the reference mirror was rotatable. In order to avoid possible effects of thermal dilation, the background spectra (reference mirror for reflectivity, hole for transmission) have been measured at the same temperature as the sample. The temperature was kept constant to within ± 2 K. The reflectivity measurements have been performed on 5-mm-thick pellets prepared from freshly precipitated AgI and pressed at 6.8 Mg/cm^2. Figure 1 shows the observed reflectivity in the β phase at 20 °C and 140 °C, and in the α phase at 170 °C, 260 °C, and 420 °C in the range between 3 and 140 cm^{-1}. The thin polycrystalline platelets used for the transmission measurements have been prepared by heating thin β-AgI single crystals into the α phase and pressing this very soft material into thin samples with thicknesses ranging between 24 and 143 μm. Normally the samples have been measured first at room temperature in the β phase and then in the α phase at different temperatures up to 440 °C. After cooling the samples to room temperature, control measurements have been performed which de-

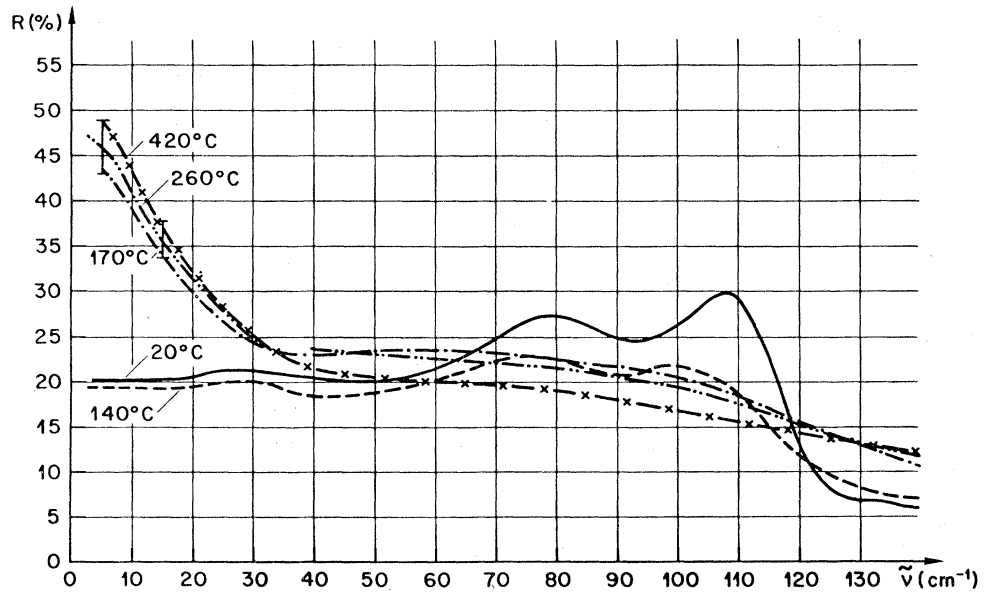

FIG. 1. Far-infrared reflectivity of β- and α-AgI at different temperatures: β-AgI, 20 °C——— ; β-AgI, 140 °C-----; α-AgI, 170 °C- · - · -; α-AgI, 260 °C- ·· - ·· -; α-AgI, 420 °C- × - × -; the β-phase → α-phase transition temperature is at 147 °C. The vertical bars at 5 and 15 cm^{-1} indicate the experimental errors.

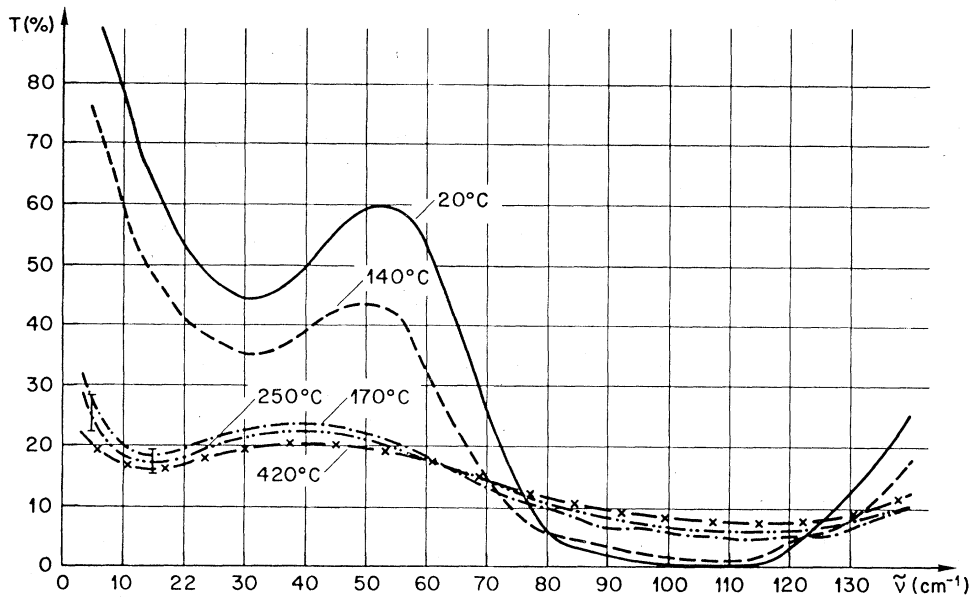

FIG. 2. Far-infrared transmission of β- and α-AgI at different temperatures; sample thickness $D = 38$ μm: β-AgI, 20 °C——; β-AgI, 140 °C-----; α-AgI, 170 °C- ·- ·- ·- ·-; α-AgI, 250 °C- ··- ··-; α-AgI, 420 °C- ×- ×-; the β-phase $\rightarrow \alpha$-phase transition is at 147 °C. The vertical bars at 5 and 15 cm^{-1} indicate the experimental errors.

monstrated that most spectra were nearly identical with the spectra before heating. This indicated that most samples survive the β-phase$\rightarrow$ α-phase transition and that no appreciable amount of iodine evaporated from the sample during heating. The transmission spectra in the β phase at 20 °C and 140 °C, and in the α phase at 170 °C, 260 °C, and 420 °C are shown in Fig. 2. The curves shown in Figs. 1 and 2 are mean curves derived from five independent measurements at each temperature. The vertical bars of the reflectivity and transmission observed at 250 °C indicate the experimental

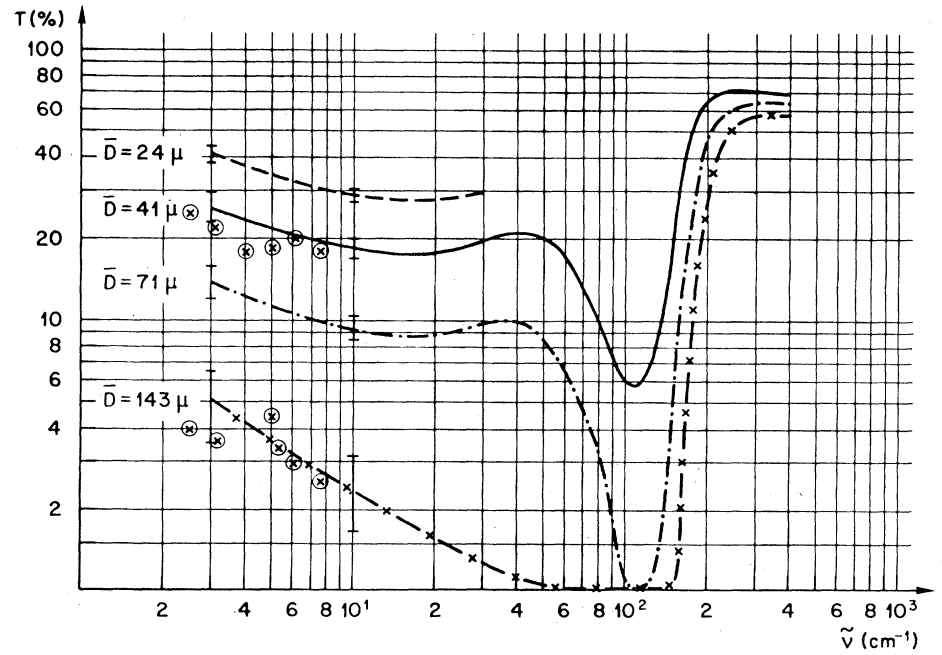

FIG. 3. Far-infrared transmission of α-AgI at 250 °C for various mean sample thicknesses $\bar{D}$: $\bar{D} = 24$ μm-----; $\bar{D} = 41$ μm——; $\bar{D} = 71$ μm- ·- ·- ·- ·-; $\bar{D} = 143$ μm- ×- ×-. The vertical bars at 3 and 10 cm^{-1} indicate the experimental errors. ⊗ microwave data.

errors. Figure 3 shows the observed transmission of α-AgI at 250 °C for different sample thicknesses $d = 24$, 41, 71, and 143 μm. The inaccuracy of the thickness is about ± 2 μm.

B. Microwave measurements

In order to check independently the far-infrared measurements, the transmission of thin samples of β- and α-AgI have been measured by microwave techniques in the frequency range between 2.5 and 8 cm^{-1}. The details of the instrument are described elsewhere.[8] A clystron generates microwave radiation with a fundamental frequency ν_0. This radiation is fed into a harmonic generator. Inside this generator, a nonlinear element has been mounted (a tungsten whisker on a semiconductor crystal) generating harmonics of ν_0. The frequency ν_0 itself is filtered out by choosing suitable dimensions for the generator's output waveguide. The unwanted radiation of the wrong harmonics is then filtered out in a simple monochromator. If necessary the frequency can be checked by a Fabry-Perot interferometer. Using three clystrons (37–42 GHz, 43–50 GHz, and 65–75 GHz) and four gratings (grating constants 2.5, 1.8, 1.0, and 0.6 mm), the region from 1.25 to 20 cm^{-1} can, in principle, be observed almost continuously. Frequencies below 2.5 cm^{-1} are obtained directly from the clystrons, omitting the harmonic generator and the monochromator.

Unfortunately, this device has one major disadvantage: It is very difficult to use it as a source for conventional spectroscopy where the frequency is scanned under fixed circumstances. The reason for this is that the source's geometry, combined with the coherent nature of its output radiation, causes a frequency-dependent standing-wave pattern in the light pipes, which cannot be corrected for. When changing the frequency, necessary adjustment of the clystron's reflector voltage and of the harmonic generator's plunger will affect this wave pattern in an unpredictable manner. To eliminate this problem, we have used a "sample-in"–"sample-out" method at fixed frequencies, rather than scanning the whole frequency range with the sample fixed. The sample is heated in vacuum inside a specially designed oven. The sample holder is a massive copper block with three cone-shaped holes of identical diameters, each of which can be placed into the light beam without changing any other circumstances; the positions of the holes in the beam are fixed by a snapping device to eliminate possible misfits. Although the three empty holes gave identical detector signals (within a few percent) when positioned in the beam, the mere presence of a sample in a hole also turned out to affect the wave pattern, giving rise to a larger spread in transmission data. This difficulty can be partly overcome by averaging the transmission data over a small frequency band around the chosen frequency. It may be minimized by using as a reference a dielectric slab of the same thickness as the sample with a well-known transmission instead of an open hole.

The transmission of the sample was determined by dividing the power passing through the sample by the power through an open hole, the frequency being fixed. The diameter of the sample was large enough to prevent diffraction effects above 2 cm^{-1}. The results of the microwave-transmission measurements are marked in Fig. 3 together with the far-infrared measurements. The agreement with the far-infrared data is reasonable, although the microwave transmission tends to be somewhat lower than the far-infrared transmission. Since the scattering in the microwave transmission is considerably larger than for the far-infrared transmission (possibly due to residual problems with standing-wave patterns), we have used the far-infrared data for the calculation of the frequency-dependent conductivity.

C. Evaluation of the frequency-dependent ionic conductivity

Normally, the optical constants are evaluated from a Kramers-Kronig analysis of the observed reflectivity R. In the case of α-AgI this is not easily possible because R is not constant at low frequencies and the necessary extrapolation towards $\tilde{\nu} = 0$ is not known (Fig. 1). Of course, one can use trial extrapolations for R and the experience has shown that in the case of α-AgI the results are not very sensitive to the different extrapolations above $\tilde{\nu} \cong 15$ cm^{-1} (Ref. 3). Below this frequency, however, a different method must be used. From combined measurements of the reflectivity R and transmission T it is possible, in principle, to determine the conductivity σ and the real part of the dielectric constant ϵ_1 as a function of frequency. Above 15 cm^{-1} where the errors of R and T are sufficiently small we have essentially applied this procedure by using the transmission data observed with the 41-μm-thick sample of Fig. 3. With the values of n and k obtained by this method we have then checked the transmission data for the other thicknesses of Fig. 3 and have found good agreement. Unfortunately, this method becomes exceedingly inaccurate below 15 cm^{-1} in the sense that small errors in R and T cause very large errors in σ and ϵ_1.

We have found that σ and ϵ_1 can be determined more accurately below 15 cm^{-1} by using only the

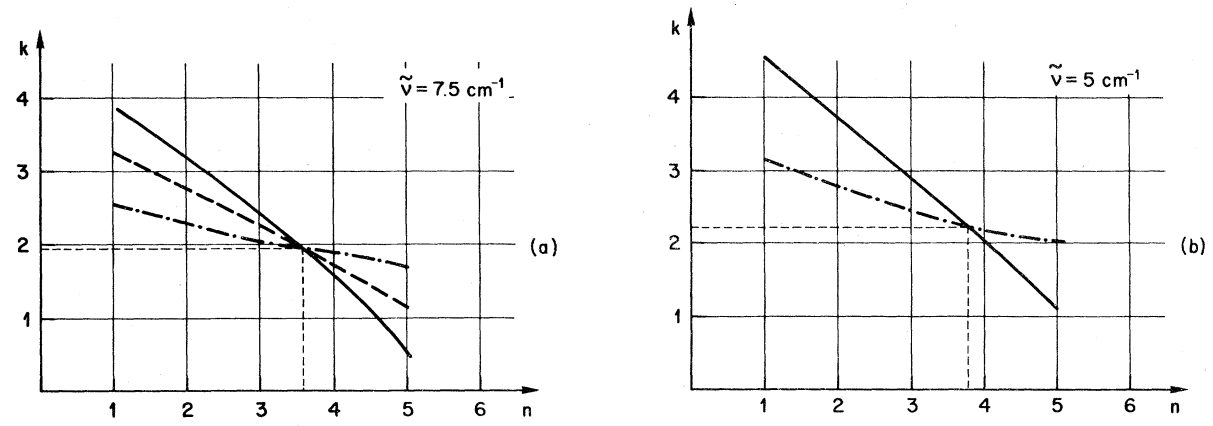

FIG. 4. (a) Determination of n and k of α-AgI at 7.5 cm^{-1} and 250 °C by the isotransmission method described in the text. $T(D=38\ \mu\text{m})=19\%$——; $T(D=70\ \mu\text{m})=9.6\%$-----; $T(D=143\ \mu\text{m})=3\%$-·-·-·-·-. (b) Determination of n and k at 5 cm^{-1} and 250 °C. $T(D=38\ \mu\text{m})=24\%$——; $T(D=143\ \mu\text{m})=4.0\%$-·-·-·-·-.

observed transmission as a function of sample thickness (Fig. 3). The transmission of a parallel platelet of thickness d is given by[9]

$$T=\frac{(1-R)^2[1+(k^2/n^2)]e^{-Kd}}{(1-Re^{-Kd})^2+4Re^{-Kd}\sin^2(\theta+\alpha)}. \tag{1}$$

Here, R is the reflectivity of a thick sample:

$$R=\frac{(n-1)^2+k^2}{(n+1)^2+k^2}, \tag{2}$$

where n is the refractive index, k the absorption constant, $K=2k\omega/c=4\pi k\tilde{\nu}$ ($\tilde{\nu}$ is the wave number, $\tan\theta=2k/(n^2+k^2-1)$, and $\alpha=2\pi nd/\lambda=2\pi nd\tilde{\nu}$. The second term in the denominator of (1) takes account of interference effects within the sample. The transmission T is a function of n, k, d, and $\tilde{\nu}$: $T=T(n,k,d,\tilde{\nu})$. For fixed $\tilde{\nu}$ and $d=d_1$ a certain value T_1 is observed. On the basis of (1) and (2) we construct an "isotransmission curve" $T(n,k,d_1,\tilde{\nu})=T_1$ in the k,n plane. Similarly, a second isotransmission curve $T(n,k,d_2,\tilde{\nu})=T_2$ can be constructed. The intersection of two (or more) isotransmission curves yields the two unknown optical constants $n(\tilde{\nu})$ and $k(\tilde{\nu})$. In order to obtain well-defined intersections, the thick-

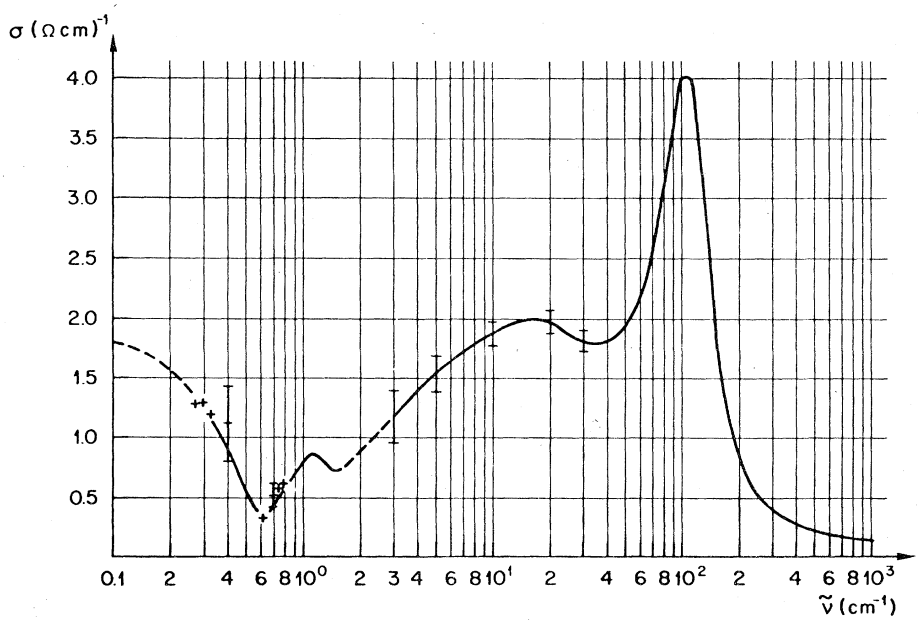

FIG. 5. Far-infrared and microwave conductivity of α-AgI at 250 °C. $\tilde{\nu}\geq 3$ cm^{-1}: our data; 0.3 cm$^{-1}\leq\tilde{\nu}\leq 1.3$ cm^{-1}: data of Ref. 1; -----inter- and extrapolations. The vertical bars indicate the experimental errors.

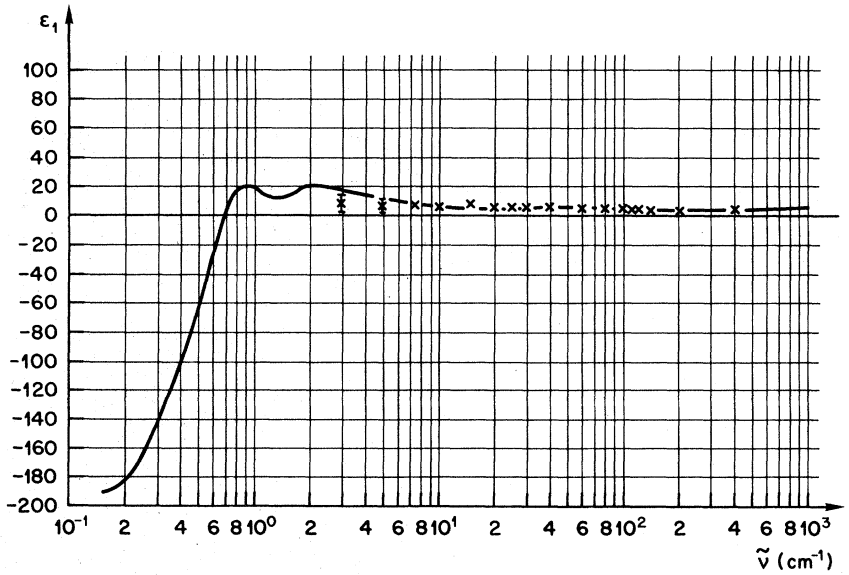

FIG. 6. Real part of the dielectric constant, $\epsilon_1(\tilde{\nu})$ of α-AgI at 250 °C. × experimental values; —— $\epsilon_1(\tilde{\nu})$ from a Kramers-Kronig analysis of $\sigma(\tilde{\nu})$ of Fig. 5 according to Eq. (3).

nesses d_1 and d_2 should be widely different. An example is shown in Fig. 4 for $\tilde{\nu} = 5$ cm^{-1} and $\tilde{\nu} = 7.5$ cm^{-1}. The conductivity is then given by $\sigma = cnk\tilde{\nu}$ and the real part of the dielectric constant is $\epsilon_1 = n^2 - k^2$. The frequency-dependent conductivity obtained by the methods described is shown in Fig. 5 together with the microwave conductivity below 1.3 cm^{-1} as observed by Funke and Eckold.[1] (Below 0.8 cm^{-1} the newer σ values of Eckold are used which are considerably lower at 0.6 cm^{-1} than the original values of Funke.) The experimentally determined dielectric constant $\epsilon_1(\tilde{\nu})$ is displayed in Fig. 6. As can be seen from the error bars in this figure, the errors in ϵ_1 are rather large below 5 cm^{-1}. In order to check the Kramers-Kronig compatibility of our experimental σ and ϵ_1 values we have calculated ϵ_1 from the conductivity at 250 °C shown in Fig. 5 by using the Kramers-Kronig relation

$$\epsilon_1(\tilde{\nu}) = \epsilon_\infty + 8\int_0^\infty \frac{\sigma(\tilde{\nu}')}{\tilde{\nu}'^2 - \tilde{\nu}^2}\, d\tilde{\nu}\,, \qquad (3)$$

where the high-frequency dielectric constant ϵ_∞ is 4.8. The results are shown in Fig. 6 (solid line). Above 7 cm^{-1} the agreement between the experimental ϵ_1 values and the Kramers-Kronig values is good; below 7 cm^{-1} the deviations are somewhat larger, which is due to the increasing experimental errors as well as to uncertainties in the inter- and extrapolations in $\sigma(\tilde{\nu})$ of Fig. 5.

III. INELASTIC NEUTRON SCATTERING EXPERIMENTS

For the first time, a single crystal of α-AgI sufficiently large for inelastic neutron scattering experiments has been grown. Pressed pellets of commercially available AgI were filled in a glass tube of approximately 1-cm diameter with narrow neck and spherical end. In consequence of the volume change in the β-α transition, the sample has to be kept above 147 °C; therefore, the crystal was grown by the Bridgemen technique directly on the neutron spectrometer. The furnace has two heating coils; after the crystal growth the upper coil was lifted in order to open a slit for the passage of the neutron beam. The whole system was mounted on a big goniometer head for the alignment of the crystal. After several trials we successfully grew a crystal of 2 cm in length, a mosaic spread of approximately 1° and a (111) orientation parallel to the scattering plane.

The inelastic neutron scattering experiments have been performed on a triple-axis spectrometer at the reactor Saphir in Würenlingen. The standard constant-$\vec{Q}$ or constant-ω scans were employed for the transversal and longitudinal modes. Pyrolitic graphite crystals were used as monochromator and analyzer in the reflecting position (002). The monochromator energy was kept fixed at 14.9 meV in conjunction with a pyrolitic graphite filter.

Most of the measurements were done at 300 °C ± 20 °C. At the end of the period, the temperature was reduced to 160 °C; however, the results did not change within experimental error.

The neutron intensity distribution of a typical constant-ω scan is shown in Fig. 7(a). The observed double maximum corresponds to the longi-

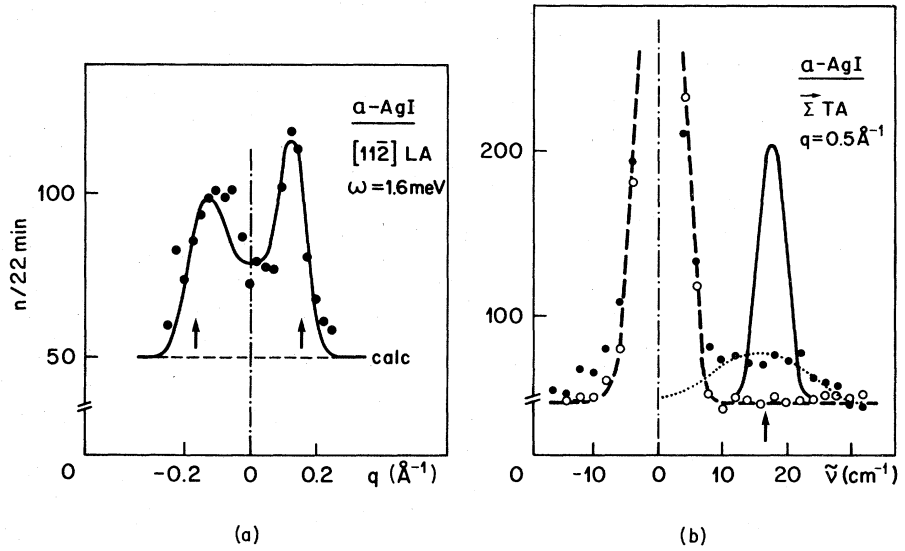

FIG. 7. Neutron scattering experiments of α-AgI. (a) Constant-ω scan. ● LA intensity; solid line: calculated intensity. Arrows mark the wave vector of the observed phonons, corrected for resolution effects. (b) Constant-$\vec{Q}$ scan. ● TA intensity; ○ background (dashed line); solid line: calculated intensity; dotted line: Gaussian fit to observed intensity; the arrow marks the observed phonon frequency.

tudinal-acoustic-phonon mode with wave vector $+\vec{q}$ and $-\vec{q}$, symmetric to the reciprocal-lattice point. The peaks are of similar energy and linewidth as those observed in the low-temperature ordered β phase.[10] Figure 7(b) displays the result of a constant-$\vec{Q}$ scan through a transverse-acoustic branch (full circles). The high intensity at zero energy transfer originates in the incoherent scattering from the glass tubes of the furnace. Open circles are the result of a scan with the same $|\vec{Q}|$, but at a point in reciprocal space where only longitudinally polarized phonons give intensity.[11] Because the longitudinal modes have a higher energy, they do not contribute in the transverse-frequency region, and therefore the open circles represent the background. The intensity difference, approximated by the dotted curve, is due to the transverse-acoustic branch; the phonon peak is smeared out and much broader than in β-AgI. The solid lines in Fig. 7 repre-

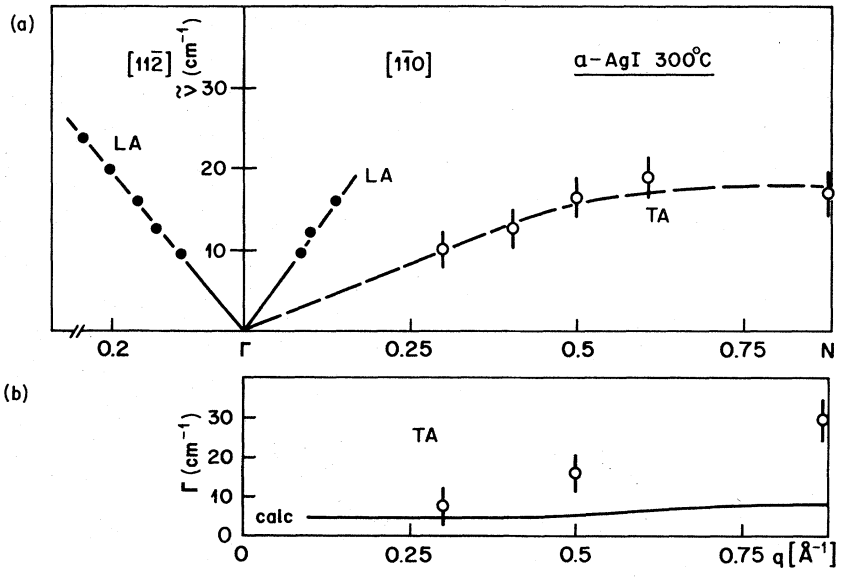

FIG. 8. (a) Observed phonon frequencies $\tilde{\nu}(\vec{q})$ in α-AgI at 300 °C; the dashed lines are a guide to the eye. (b) Linewidth $\Gamma(\vec{q})$ for the [110] TA mode; the solid line represents the calculated width (mosaic spread included).

sent the calculated intensity distribution, based on the convolution of the spectrometer resolution function with an energetically sharp excitation function. The mosaic of the sample has been taken into account by representing the dispersion curve by a band of frequencies whose angular spread was adjusted to the experimental resolution measured at the Bragg points. For the longitudinal modes [Fig. 7(a)] the experimental and theoretical intensity distributions agree fairly well, whereas a large discrepancy is observed for the transverse modes [Fig. 7(b)]. Figure 8 displays the experimentally determined phonon dispersion of the acoustic modes of α-AgI. The dahsed lines are a guide to the eye. The frequencies are slightly softer than those in β-AgI. The linewidth of the [110] TA phonons is shown at the bottom of Fig. 8. The open circles give the observed linewidth. The calculated linewidth, based on the above-mentioned procedure is represented by the solid line and is much smaller than the observations. Only part of the LA modes have been detemined, and the optic modes have not been measured at all. This limited information is due to the following physical reasons: (i) Instrinsically strong anharmonicity of the silver halides, observed in β-AgI (Ref. 10) as well as in AgCl (Ref. 12) and AgBr (Ref. 13), making feasible a complete phonon-dispersion measurement only at very low temperatures, and (ii) very large Debye-Waller factor for α-AgI (Ref. 14); as a consequence, in the inelastic coherent cross section[11] the exponential decrease e^{-W} always dominates the $\hbar^2Q^2$ term, leaving only a few reciprocal-lattice vectors useful for a scattering process.

IV. DISCUSSION

A. Optical properties in the far infrared

1. Far-infrared properties of β-AgI

In β-AgI we observe the main residual-ray absorption near 110 cm^{-1} (Figs. 1 and 2) corresponding to the $\vec{q}=0$ TO modes of symmetry A_1 and E_1. The origin of this main absorption band is well understood; it corresponds to the vibration of the Ag ions against the I ions; with increasing temperature this mode becomes highly damped which reflects the strong anharmonicity in this compound.[15,16] In the vicinity of the β-phase $\rightarrow\alpha$-phase transition an anomalous damping has been observed which might be related with thermally activated silver ions.[17]

Although this paper is mainly devoted to α-AgI, we take the opportunity to discuss here some features of β-AgI, which are still not yet completely understood. This concerns the question as to the origin of the additional structures observed in the far-infrared[15-18] and Raman spectra[19-24] in the regions near 80 and 30 cm^{-1}. There are two possible explanations for this subsidiary structures: (1) One explanation is interpretation in terms of multiphonon processes; here one assumes a perfectly ordered but anharmonic crystal. Anharmonicity will couple different phonons and if the $\vec{q}$-selection rules as well as the specific selection rules for infrared and Raman activity are satisfied, such processes can produce additional structures, especially if phonons at critical points in the Brillouin zone are involved for which the combined density of states is large.[25] (2) An interesting alternative interpretation is based on a harmonic but disordered crystal; the defects will break the $\vec{q}$ selection rules to some extent and allow phonons that occur throughout the Brillouin zone to be observed.[4,21,22] We first consider the experimental situation and then discuss the results in terms of the two models mentioned above.

In the far-infrared reflectivity spectrum (Fig. 1) the 80-cm^{-1} structure is clearly resolved, but in the transmission spectrum (Fig. 2) it is completely hidden by the main absorption band. In thinner samples, however, this structure can also be observed in transmission.[18] With decreasing temperature the intensity of the peak decreases and its frequency increases: A two-oscillator fit gives a peak frequency of 84 cm^{-1} at 145 K (Ref. 15) while a Kramers-Kronig analysis of the reflectivity of single crystals yields a peak frequency of 87 cm^{-1} in $\epsilon_2(\tilde{\nu})$ at 193 K (Ref. 16). A similar structure near 85 cm^{-1} has also been observed in the Raman spectra[19-24] and shows qualitatively the same temperature dependence as the corresponding infrared structure: At 80 K the intensity of this structure is considerably weaker than at room temperature and its frequency is 94 cm^{-1} (Ref. 19). The second subsidiary structure is observed in the transmission spectrum of Fig. 2 near 32 cm^{-1}. Applying Eq. (1) it is found that this structure is attributed to a great extent to interference effects within the sample. Only a weak resonance in $\sigma(\tilde{\nu})$ and $\epsilon_2(\tilde{\nu})$ remains near 40 and 35 cm^{-1}, respectively.[7] That this resonance is in fact intrinsic is also indicated by the very weak structure observed in the reflectivity spectrum in this frequency range (Fig. 1). Again, there exists a corresponding Raman line with a frequency between 37 and 40 cm^{-1} at room temperature[19-24]; the intensity of this line is considerably weaker at 80 K and its frequency increases to 47 cm^{-1} (Ref. 19).

We now propose our interpretation in terms of two-phonon processes. From its temperature de-

pendence the far-infrared structure near 80–90 cm^{-1} has been tentatively assigned to a TA+LA zone-boundary combination mode which is infrared active.[15] This assignment is strongly supported by inelastic neutron scattering experiments which yield zone-boundary TA and LA phonons with frequencies of 15 and 74 cm^{-1}, respectively, at the M point at 160 K (Ref. 10). A group-theoretical analysis shows that a similar assignment is possible for the corresponding Raman structure.[26-28] As to the second structure near 35 cm^{-1} we suggest that it originates from two-phonon processes involving pairs of TO phonons with opposite wave vectors and with frequencies between 15 and 20 cm^{-1}. TO-phonon branches with very weak dispersion and correspondingly high density of states have indeed been observed in this frequency range in the Δ and Σ directions of the Brillouin zone.[10] An example is the combination of two TO phonons at the M point with a frequency of 20 cm^{-1} which is infrared and Raman active.[26,27]

We now turn to the second interpretation which is based on defects and has been proposed by Burns[21] and Alben and Burns.[4] Two kinds of defects are considered: The first kind are thermally activated (Frenkel) defects which give rise to the observed ionic conductivity of the silver ions.[21] This interpretation is qualitatively compatible with the temperature behavior of the extra lines. On the other hand, the concentration of Frenkel defects is quite small, less than 4% at 140 °C (Ref. 14) and it is difficult to understand how such a small defect concentration can give rise to comparatively strong structures in the Raman spectra. In addition, two-phonon processes of the type discussed above have also been observed in other compounds with wurtzite structure, such as CdS (Refs. 29 and 30) and ZnO (Ref. 31) which are not known to have appreciable ionic conductivities. It is important to note that in the case of CdS the intensities of the two multiphonon Raman lines with lowest frequencies are larger than those of the fundamentals at room temperature,[29] a situation which is similar to that of β-AgI. As to the second kind of defects, small statistical displacements of all the silver ions from their tetrahedral positions are assumed.[4] Alben and Burns have indeed shown by quantitative calculations that these defects give rise to structures near 80 cm^{-1} in both the infrared and Raman spectra, but not near 40 cm^{-1} (Ref. 4). Some support for this view is given by the Raman study of Fontana *et al.*[24] who in contrast to other authors[17,19,20] claim that the extra lines are not ordinary second-order peaks and infer the possibility of a first-order partial disordering in the Ag sublattice at about 50 K. Unfortunately, the displacement order assumed in the second interpretation is at least controversial[32-34] and could not be confirmed by more recent structural studies.[14] At the moment, no definite conclusions can be drawn as to the origin of these extra lines. It is possible that both anharmonicity as well as disorder are involved, the latter mainly in the vicinity of the β-phase$\rightarrow\alpha$-phase transition, and it is also possible that these two mechanisms can not even be clearly separated. For the reasons discussed above we believe that the dominating mechanism is anharmonicity. That anharmonicity is of fundamental importance in β-AgI has been demonstrated by a number of papers[10,14-16,19]

2. *Far-infrared properties of* α-AgI

Heating the sample across the order-disorder phase-transition at 147 °C results in a drastic change of the transmission spectrum (Fig. 2). The main absorption band near 110 cm^{-1} survives the phase transition but becomes extremely smeared out. The drastic decrease in the transmission below about 60 cm^{-1} is accompanied by a corresponding increase in the reflectivity in this region (Fig. 1). Although the temperature dependence of the reflectivity and transmission is weak in the α-phase (Figs. 1 and 2), the main absorption near 110 cm^{-1} still shows some increase in damping if the temperature is raised from 170 °C to 420 °C. This can be seen from the peak values of the main resonance of $\sigma(\tilde{\nu})$ which decrease with increasing temperature. Based on the data of Figs. 1 and 2 and with the help of Eqs. (1) and (2) we obtain peak values of 4.4, 4, and 3.4 $(\Omega\,\mathrm{cm})^{-1}$ at 170 °C, 250 °C, and 420 °C, respectively. The value of 4.4 $(\Omega\ \mathrm{cm})^{-1}$ from our present data at 170 °C is in fair agreement with the value of 4.8 $(\Omega\,\mathrm{cm})^{-1}$ from our earlier measurements performed at 180 °C (Ref. 16); the discrepancy of 9% is due to different sample preparation and measurement techniques as well as to different evaluation procedures applied in the two cases. In view of the progress made in the meantime, our new data are more accurate than the older ones. There remains still a discrepancy between our data at 250 °C with a peak value of 4 $(\Omega\,\mathrm{cm})^{-1}$ as compared to the value of 3.3 $(\Omega\ \mathrm{cm})^{-1}$ observed by Funke and Jost at the same temperature.[1] However, more recent studies of Funke *et al.* have shown that their earlier value is indeed too low and that our value is appropriate.[35] This implies that the frequency-dependent conductivity obtained indirectly from Raman measurements[4,21,22] and which has been normalized to the peak value of Funke and Jost should be renormalized to our peak value at the appropriate temperature.

More important than the absolute peak values of the main absorption band is the question as to the strong far-infrared absorption observed in α-AgI in the region between about 60 and 7 cm^{-1}. In contrast to β-AgI, where according to our opinion the additional structures are mainly due to anharmonicity, we agree here with Alben and Burns[4] that this absorption in α-AgI is mainly due to disorder. This is indicated by the drastic change of the transmission at the order-disorder transition temperature and its relatively weak temperature dependence in the α phase (Fig. 2). That the degree of disorder does not change appreciably with temperature in the α phase has been shown by recent elastic neutron scattering experiments[14,36] as well as by configurational model calculations based on the disorder entropy[37]; this implies only a weak temperature dependence of the disorder-induced absorption. The disorder of the silver ions in α-AgI will break the selection rules[4] and we expect a coupling of the high-frequency infrared-active TO modes near 110 cm^{-1} with all first-order low-frequency modes, the nature of which will be discussed in more detail in Sec. IV B. This coupling is associated with a transfer of oscillator strength of the high-frequency TO modes to the low-frequency modes which results in the observed strong absorption. A more quantitative study of the disorder-induced absorption of α-AgI has been given recently by Alben and Burns[4] and by us.[5] Alben and Burns have calculated the phonon density of states, the reduced Raman intensity and the far-infrared conductivity based on the equation-of-motion method for a large cluster containing about 250 unit cells of different configurations for the silver ions. Our approach is quite different[5]; in a first step we constructed a dynamical matrix for the primitive unit cell of a virtual crystal. The fluctuations of the force constants with respect to this virtual crystal are then introduced and the problem is treated using a coherent-potential-approximation method. Both models are able to account qualitatively for the observed far-infrared conductivity above 10 cm^{-1} (Fig. 5).

At very low frequencies, below about 5 cm^{-1}, a strong temperature dependence of the transmission is expected because in this range the diffusion-controlled regime is approached and anharmonicity becomes more important. The data of Fig. 2 indeed show that in this region the temperature dependence of the transmission becomes stronger and imply an increasing conductivity with increasing temperature in agreement with the microwave data.[1] Figure 5 also shows that our absolute values of $\sigma(\tilde{\nu})$ between 5 and 3 cm^{-1} extrapolate reasonably well to the microwave data of Funke and Jost between 1.3 and 0.3 cm^{-1} (Ref. 1).

B. Inelastic neutron scattering experiments

The intepretation of the inelastic neutron-scattering experiments as shown in Fig. 8 is based on a comparison of the data of α-AgI and β-AgI, e.g., a disordered crystal at high temperature (300 °C) and an ordered crystal at room temperature and at 160 K (Ref. 10). In α-AgI, the longitudinal-acoustic modes could be measured up to 3 meV (24 cm^{-1}). At higher energies, the peaks were smeared out due to anharmonic effects. This energy is a reasonable continuation of β-AgI, where the limit was 5 meV (40 cm^{-1}) at room temperature. Thus, the LA compressional modes show a normal temperature-dependent anharmonicity and no drastic change is observed at the order-disorder transition. This is in sharp contrast to the TA-shearing modes: In the β phase we mesure well-defined phonon peaks, whereas in the α phase the linewidths are very large, about 4 meV (32 cm^{-1}) at the zone boundary, which is about twice the mean energy (Fig. 8). In a well-ordered crystal such as β-AgI where the line broadening is due to anharmonicity, the TA modes are usually better defined than the LA modes. In α-AgI the situation is reversed; if the very large linewidths of the TA modes would be entirely due to anharmonicity, we would expect that the LA modes would be smeared out to such an extent that they would be unobservable. From this different behavior of the modes we conclude that it is mainly the disorder which is responsible for the extremely large linewidths of the TA modes in α-AgI.

In order to account for disorder, we have performed preliminary lattice-dynamical calculations based on the four different configurations of the two silver ions in the cubic unit cell shown in Fig. 9. The same force constants as those of β-AgI have been used.[10]

Configuration 1 gives a satisfactory agreement with the observed LA modes and the mean frequencies of the TA mode as well as for the optic modes in the region of the strong infrared absorption near 110 cm^{-1}. The other three configurations differ by about 25% for the LA frequencies, e.g., a 5-cm^{-1} spread at the energy of 20 cm^{-1}. The calculated TA frequencies on the other hand vary by about 60% (6 cm^{-1}) at $q = 0.5$ $Å^{-1}$ and 80% (16 cm^{-1}) at the zone boundary. Thus, our proposed model accounts well for the small and broad bandwidth of the longitudinal and transversal phonons, respectively.

Inspection of the calculated eigenvectors of the TA zone-boundary modes show that the displacements of the ions are such that little or no

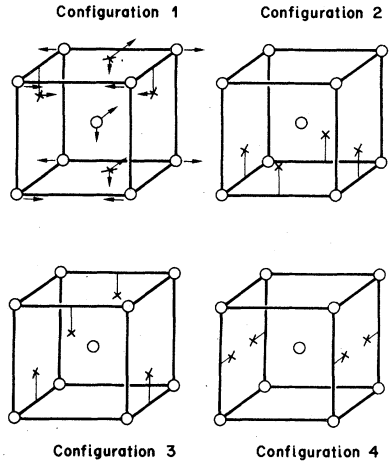

FIG. 9. Four different configurations of the silver ions in the cubic unit cell of α-AgI. All configurations with two silver ions in nearest-neighbor sites are excluded. The statistical weight of configuration 1 is four, that of configurations 2, 3, and 4 is one only. ○ iodine ions, × occupied silver sites. The arrows in configuration 1 indicate the eigenvector of the [110] TA–zone-boundary mode with a calculated frequency of 20 cm^{-1}.

changes occur in the nearest Ag–I and I–I distances, thereby minimizing the mutual repulsion between the ions (Fig. 9). This kind of motion favors the jump of silver ions into neighboring empty sites, and the mode illustrated in configuration 1 of Fig. 9 represents a *reaction coordinate* for such jumps.

The above results are obtained from lattice-dynamical calculations based on perfectly ordered crystals. As has already been emphasized by Alben and Burns, in reality disorder will break the $\vec{q}$ selection rules,[4] but locally, low-frequency modes of the type described above will still exist although they will now couple to all other modes resulting in a large spread of vibrational frequencies. Owing to disorder these local modes will gain oscillator strength, which explains the high conductivity of α-AgI below 30 cm^{-1} (Ref. 4). It should be pointed out that there is a close connection between the optical and the neutron scattering experiments: The high conductivity below 30 cm^{-1} implies a high density of states down to about 3–5 cm^{-1}. The phonons which produce this high density of states are just the TA phonons observed by inelastic neutron scattering, in particular the zone-boundary modes with frequencies ranging between about 5 and 30 cm^{-1}. In summary, the existence of these low-frequency modes is now clearly established by far-infrared and Raman as well as neutron scattering experiments.

ACKNOWLEDGMENTS

We would like to thank Dr. H. U. Beyeler, Dr. S. Strässler, and Dr. H. R. Zeller for helpful discussions and Mr. W. Foditsch for his never-ending patience in preparing AgI samples as well as for his skilled technical assistance during the measurements.

[1]K. Funke and A. Jost, Ber. Bunsenges. Phys. Chem. 75, 436 (1979); G. Eckold, thesis, Göttingen, 1975 (unpublished).
[2]K. Funke, Prog. Solid State Phys. 11, 345 (1976).
[3]P. Brüesch, L. Pietronero, S. Strässler, and H. R. Zeller, Phys. Rev. B 15, 4631 (1977).
[4]R. Alben and G. Burns, Phys. Rev. B 16, 3746 (1977).
[5]H. U. Beyler, P. Brüesch, L. Pietronero, W. R. Schneider, S. Strässler, and H. R. Zeller, in *Topics in Current Physics*: *The Physics of Superionic Conductors*, edited by M. B. Salamon (Springer, New York, 1979), Vol. 15, p. 77.
[6]D. H. Martin and E. Puplett, Infrared Phys. 10, 105 (1969).
[7]P. Brüesch and W. Foditsch, J. Phys. E 12, 872 (1977).
[8]M. J. Huyben, C. G. C. M. de Kort, J. H. M. Stoelinga, and P. Wyder, Infrared Phys. 19, 257 (1979).
[9]D. L. Greenaway and G. Harbeke, in Int. Ser. Monogr. Sci. Solid State 1, 8 (1968).
[10]W. Bührer, R. M. Nicklow, and P. Brüesch, Phys. Rev. B 17, 3362 (1978).
[11]G. Dolling, in *Dynamical Properties of Solids*, edited by G. K. Horton and A. A. Maradudin (North-Holland, Amsterdam, 1974), 1, 541 (1974).
[12]P. R. Vijayaraghavan, R. M. Nicklow, H. G. Smith, and M. K. Wilkinson, Phys. Rev. B 1, 4819 (1970).
[13]Y. Fujii, S. Hoshino, S. Sakuragi, H. Kanzaki, J. W. Lynn, and G. Shirane, Phys. Rev. B 15, 358 (1977).
[14]R. J. Cava, F. Reidinger, and B. J. Wuensch, Solid State Commun. 24, 411 (1977).
[15]A. Hadni, J. Claudel, and P. Strimer, Appl. Opt. 7, 1159 (1968).
[16]P. Brüesch, S. Strässler, and H. R. Zeller, Phys. Status Solidi A 31, 217 (1875).
[17]M. Peyrad and J. P. Misset, Solid State Commun. 17, 1487 (1875).
[18]G. L. Bottger and A. L. Geddes, J. Chem. Phys. 46, 3000 (1967).
[19]G. L. Bottger and C. V. Damsgard, J. Chem. Phys. 57, 1215 (1972).
[20]R. C. Hanson, T. A. Fjeldly, and H. D. Hochheimer, Phys. Status Solidi B 701, 567 (1975).
[21]G. Burns, F. H. Dacol, and M. W. Shafer, Solid State Commun. 19, 291 (1976).
[22]G. Burns, F. H. Dacol, and M. W. Shafer, Phys. Rev. B 16, 1416 (1976).
[23]M. J. Delaney and S. Ushioda, Solid State Commun. 19, 297 (1976).
[24]A. Fontana, G. Mariotto, M. Montagna, V. Capozzi, E. Cazzanelli, and M. P. Fontana, Solid State Com-

mun. 28, 35 (1978).
[25]H. Bilz, in *Phonons in Perfect Lattices and Lattices with Point Imperfections*, edited by R. S. W. Stevenson (Plenum, New York, 1966), p. 208; R. Loudon, Adv. Phys. 13, 423 (1964).
[26]M. A. Nusimovici and J. L. Birman, Phys. Rev. 156, 925 (1968).
[27]M. A. Nusimovici, M. Balkanski, and J. L. Birman, Phys. Rev. B 1, 595 (1970).
[28]J. J. Sullivan, J. Phys. Chem. Solids 25, 1039 (1964).
[29]B. Tell, T. C. Damen, and S. P. S. Porto, Phys. Rev. 144, 771 (1966).
[30]H. W. Varleur and A. S. Barker, Phys. Rev. 155, 750 (1967).
[31]T. C. Damen, S. P. S. Porto, and B. Tell, Phys. Rev. 142, 570 (1966).
[32]L. Helmholtz, J. Chem. Phys. 3, 740 (1935).
[33]B. R. Lawn, Acta Crystallogr. 17, 1341 (1964).
[34]G. Burley, J. Chem. Phys. 38, 2807 (1963).
[35]K. Funke, private communication.
[36]A. F. Wright and B. E. F. Fender, J. Phys. C 10, 2261 (1977).
[37]H. U. Beyeler and S. Strässler, Phys. Rev. B 20, 1980 (1979).